Journal of Information Systems Engineering and Management
2025, 10(4)
e-ISSN: 2468-4376
https://www.jisem-journal.com/

Research Article

Data-Driven Prediction of Swirling Flow Fields via Feedforward Backpropagation Neural Networks

Messaoud Bendaoui[1], Abdessalam Kifouche[2], Djemoui Lalmi[3,6,*], Fadila Barkat[4], Khadidja Khodja[5], Redjem Hadef[6]

[1]*Faculté de Technologie, Département de socle commun ST Université de Batna 2 Algeria*
[2]*Laboratoire de l'énergie et des systèmes intelligents LESI, Departement génie electrique, Faculté des Science et de la technologie, Université de Khemis Miliana, Algérie, Algeria*
[3]*Laboratory of Materials, Energy Systems Technology and Environment, Faculty of Sciences Technology, Departement of Automatics and electromechanics, University of Ghardaia, Algeria*
[4]*University of Ghardaia BP 455 Ghardaia 47000, Algeria*
[5]*Centre de Développement des Energies Renouvelables, CDER, Algérie, Algeria*
[6]*Departement génie mécanique, Université l'Arbi ben M'hidi, Oum el Bouaghi, Algeria*

**Corresponding author Email: lalmi.djemoui@univ-oeb.dz*

ARTICLE INFO

Received: 25 Dec 2024
Revised: 21 Sep 2025
Accepted: 20 Nov 2025

ABSTRACT

Improving energy efficiency while minimizing environmental impact has long been a central challenge in combustion-based technologies. Swirl (vortex) flow, a key innovation for enhancing combustion, remains an active research focus. This study explores the use of artificial intelligence to predict swirl flow characteristics in a combustion chamber. Experimental positional and descriptive data served as inputs, with horizontal and vertical velocities and kinetic energy as outputs. The model accurately reproduced velocity density distributions and vortex center locations, closely matching experimental results. It demonstrated strong predictive performance on known datasets, effective reconstruction of the vortex flow field, and robust generalization to unseen cases. These results confirm AI's potential for modeling complex combustion flows and suggest promising applications for predictive control and optimization in energy systems.

Keywords: Swirling flow, neural network, recirculation zone, training, validation, test and prediction.

INTRODUCTION

Swirling flows, characterized by the rotational motion of fluid particles around a central axis, manifest in a multitude of engineering and natural systems, exerting a profound influence on their performance and behavior(Syred, 2006). From the efficient mixing in industrial processes to the optimization of combustion in propulsion systems, and from the dynamics of oceanic currents to the dispersion of pollutants in the atmosphere, understanding the intricate behavior and characteristics of swirling flows is paramount for a diverse array of applications(Sheen et al., 1996). However, traditional methods of analyzing swirling flows have often been constrained by their reliance on empirical correlations derived from limited experimental observations.

The advent of artificial intelligence (AI) heralds a new era in the study of swirling flow phenomena, offering unprecedented opportunities to enhance our understanding and predictive capabilities(Schmittel et al., 2000). By harnessing AI techniques, particularly machine learning algorithms, researchers can unlock hidden patterns and relationships embedded within vast datasets of swirling flow simulations and experimental measurements(O'Doherty&Lucca-Negro, 2001).

This approach transcends the limitations of traditional methods, empowering scientists and engineers to develop predictive models that capture the dynamics of swirling flows with unparalleled accuracy.

This interdisciplinary fusion of fluid dynamics principles with AI methodologies holds immense promise for advancing the characterization of swirling flows. Through the deployment of advanced machine learning algorithms such as neural networks, genetic algorithms, and reinforcement learning, this study endeavors to delve deep into the complexities of swirling flow dynamics. By analyzing intricate flow structures, turbulence characteristics, and vortex dynamics,

Journal of Information Systems Engineering and Management
2025, 10(4)
e-ISSN: 2468-4376
https://www.jisem-journal.com/

Research Article

researchers aim to unravel the underlying mechanisms governing swirling flows across diverse spatial and temporal scales(Mathur&NR, 1967).

The outcomes of this research transcend disciplinary boundaries, with profound implications for fields ranging from aerospace engineering to energy production and environmental science. By gaining deeper insights into swirling flow phenomena through the lens of artificial intelligence, engineers and scientists can revolutionize the design of more efficient and sustainable technologies, optimize fluidic processes, and mitigate environmental impacts(Leuckel&Fricker, 1976).

Moreover, the knowledge derived from this study contributes to the advancement of fundamental fluid dynamics principles, laying the groundwork for future innovations in flow control, turbulence modeling, and renewable energy systems(Guedot, 2015).

In summary, the integration of artificial intelligence into the characterization of swirling flows marks a transformative paradigm shift in fluid dynamics research. By harnessing the computational power and analytical prowess of AI-driven methodologies, researchers stand poised to unlock unprecedented insights into the complexities of fluid motion, driving innovation and progress across a myriad of engineering and scientific domains.

This study aims to utilize one of the artificial intelligence models to predict the characteristics of swirling flow. The research focuses on integrating state and spatial parameters to estimate the axial and radial components of velocity, as well as turbulent kinetic energy. The reliability of the model is assessed using statistical parameters such as the error between predicted and measured values, MSE (Mean Squared Error), and RMSE (Root Mean Squared Error).

Material and method

Many industrial processes use vortex flows to improve combustion because the vortex flow field generated by the head vortex directly affects the uniformity of fuel and air mixing, and thus the quality of the temperature distribution at the combustion outlet, the formation of the internal recirculation zone allows high volumetric heat release rates in conjunction with Excellent flame stability(Escudier&Keller, 1985).

Introducing swirling air through two or more concentric rings provides additional degrees of freedom to control the radial distribution of flow and vortex to achieve significantly different combustion characteristics, such as flow and mixing patterns, turbulence levels, and different flame stability limits. Therefore, for combustion design, it is very important to obtain a clear picture of the characteristics of the vortex flow field.

To research the fields of vortex flow and study its characteristics, use one of the artificial neural network models, which focuses on integrating state parameters and spatial parameters to estimate the axial and radial components of the velocity, in addition to turbulent kinetic energy, and compare the expected and measured values by measuring the error rate (R, R^2, MSE) to evaluate the reliability of the model(Elattar et al., 2020).

Generic Model Combustor

The experiments were carried out using an atmospheric air blast atomizer in a cylindrical combustion chamber (Merkle et al., 2003). The atomizer consists of a modular arrangement of two radial swirl generators, an atomizer lip that separates the two airstreams from each other within the nozzle, and an air diffuser with a throat diameter of $D_0=2R_0=25$ mm.

For both airflows, a constant air preheat temperature of $T_0= 50$ °C has been selected. The mass flow rate of air is adjusted to 64 kg/h ($M_i/M_0=0.37$). Theoretical swirl numbers S_0, the of the inner as well as the outer airflow are $S_i=0.46$ and $S_0=1$, resulting in a global swirl number of 0.81. The Reynolds number is calculated as the product of the axial average air velocity at the nozzle exit (39.9 m/s) and the throat diameter of the diffuser divided by the kinematic viscosity of the air and yields approximately 60,000.

Journal of Information Systems Engineering and Management
2025, 10(4)
e-ISSN: 2468-4376
https://www.jisem-journal.com/

Research Article

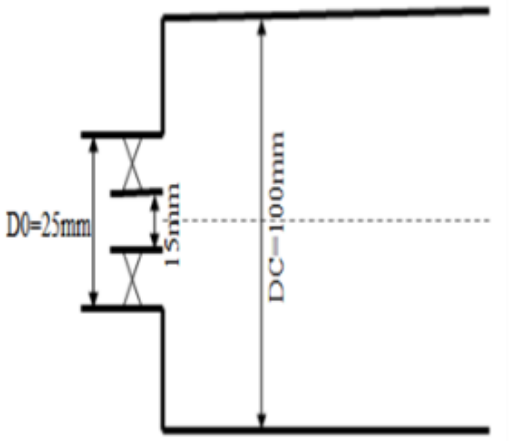

Figure 1: Generic Model Combustor

Measurements of the position and state parameters of the vortex flow field inside the combustion chamber were made using a sensor. Record the experimental values in a table.

Include data:

- Column 1: Height h.
- Column 2: Radius R.
- Column 3: Axial velocity u.
- Column 4: Radial velocity v.
- Column 5: Tangential velocity w.
- Column 6: Kinetic energy k.

Proposed feed-forward back propagation network (ffbpn) approach

Several factors can be considered for model development that have a greater impact on the vortex flow state (recirculation zones). The proposed methodology began by collecting a dataset from a general model of combustion. Six parameters were determined, and these samples were taken as input to the FEBN model to extract vortex flow field characteristics(Zabihi et al., 2019). The FFBPN technique was used to train the performance model from two-way iterations. The first method involves calculating the forward step of the input weights and the second method is calculating the reverse step to update the weights and calculate the errors. Seventy percent of the collected data was used to train the model, while 30% of the data was divided equally for testing and 15% for validation. The overall methodology is presented in Figure.III.2:

Secondly, the model was trained based on Equation (III.1) to generate more accurate output values:

$$y(k) = F(\sum_{i=1}^{m} w_i . x_i + b) \quad (1)$$

former Where $y(k)$ e variable, x_i is the initial value of the variable and is the value of the connection weight of the neuron, and b is biased. The activation function between the input and the hidden layer was “SIGMOID”, as shown in Equation (2).

$$F(x) = \frac{1}{e^{-\mu x}} \quad (2)$$

Journal of Information Systems Engineering and Management
2025, 10(4)
e-ISSN: 2468-4376
https://www.jisem-journal.com/

Research Article

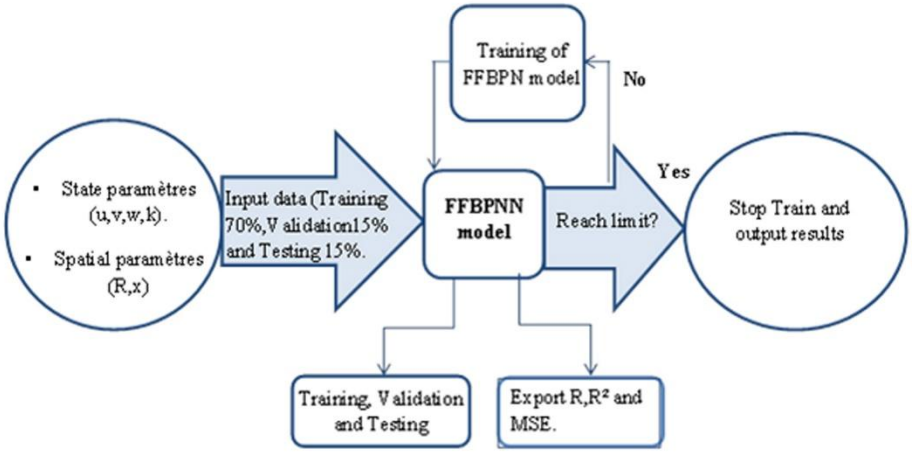

Figure 2: FFBPN approach workflow

MATLAB was used to develop the FFBPN model. During the initial training phase, the FFBPN-based model is trained using the available data. If the model fails to meet expectations, it allows the weight and bias updating process to be continuously redeployed and improved until it reaches the best requirements using the Levenberg-Marquardt (LM) backpropagation algorithm(Moayedi et al., 2020). After completing the model training, 15% of the data was used to validate the trained model in the validation phase. The model was also allowed to go through the testing phase and tested with the remaining 15% of the data sets, and the results were accurate when the R^2 value approached 1. This network consists of three layers, i.e. the input layer, the hidden layers, and the output layer.

-Input layer: The input layer consists of a group of neurons whose number is equal to the number of inputs that we will rely on and we will take as inputs the axial velocity u, radial velocity v, tangential velocity w, radius R, length h and kinetic energy k. If the goal is to predict the axial velocity u, the input is (R.h.v.w.k), but if the goal is to predict the radial velocity v, the input is (R.h.u.w.k). As for the kinetic energy K, the input (R.h.u.v.w). The neural network learns the characteristics of the input data for later use in the prediction process, so the number of neurons in the input layer will be 5.

-Hidden layer: The hidden layer consists of a group of hidden layers, and their number is determined according to the type of study and the number of inputs, their number is often small, so in this model, we will rely on ten (10) hidden layers, but as for the number of hidden neurons, it is variable.

-Output layer: Since the goal of the study is to predict the axial velocity u, radial velocity v, or kinetic energy k in the vortex flow, the output layer consists of a single neuron.

Thus, the structure of the neural network used will be as shown in Fig3:

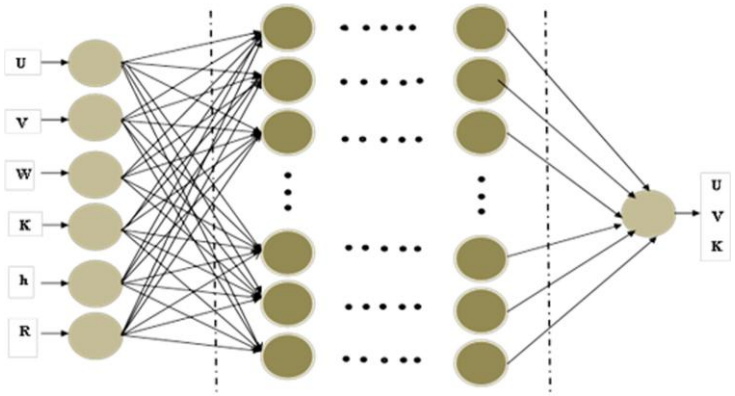

Figure 3: The structure of the neural network

Journal of Information Systems Engineering and Management
2025, 10(4)
e-ISSN: 2468-4376
https://www.jisem-journal.com/

Research Article

RESULTS AND DISCUSSIONS

FFBPNN Model Training, validation, and testing

To determine the FFBPNN framework for eddy flow field prediction in this study, it is necessary to compare and analyze the prediction accuracy, goodness of fit, and training cost of models with different hidden neurons and thus determine the optimal number of hidden neurons(Shaik et al., 2020).

An FFBPN neural network is developed to predict well the axial velocity u, radial velocity v, and kinetic energy k of vortex flow. Due to the availability of limited data, specific factors were considered as inputs to develop the model. The model developed was trained based on equation and Levenberg-Marquardt backpropagation algorithm; the model was subsequently validated and tested by providing all possible datasets. The MSE is used to characterize the error between the FFBPN-predicted value and the experimental value. The goodness of fit between the FFBPN-predicted value and the experimental value is quantitatively evaluated by the coefficient of determination R^2, the greater the value of R^2 within the range [0, 1], the better the goodness of fit. R^2 and MSE are given by the following expression:

$$R^2 = 1 - \frac{\sum_{i=1}^{n}(y_{inp} - y_{otp})^2}{\sum_{i=1}^{n}(y_{inp} - \bar{y}_{inp})^2} \quad (3)$$

$$MSE = \frac{1}{n}\sum_{i=1}^{n}(y_{inp} - y_{otp}) \quad (4)$$

The overall R^2 and MSE values changed mostly as the number of hidden neurons varied, ranging from a minimum of 14 to a maximum of 28, as shown in Table 1.

Table 1. Overall R^2 and MSE values versus several hidden neurons

No. of Neurons	Axial velocity u		Radial velocity v		Kinetic energy k	
	MSE	R^2	MSE	R^2	MSE	R^2
14	7.11×10^{-4}	0.99701	4.824×10^{-4}	0.99576	1.6×10^{-3}	0.99535
15	10^{-3}	0.99562	1.2×10^{-3}	0.98975	1.139×10^{-4}	0.93471
16	8.124×10^{-4}	0.99659	6.435×10^{-4}	0.99437	1.5×10^{-3}	0.99472
17	9.116×10^{-4}	0.99622	4.224×10^{-4}	0.99626	1.32×10^{-4}	0.97223
18	1.7×10^{-3}	0.99327	7.119×10^{-4}	0.99371	6.976×10^{-4}	0.98474
19	5.894×10^{-4}	0.99752	2.494×10^{-4}	0.99779	3.706×10^{-4}	0.97914
20	1.3×10^{-3}	0.99432	9.113×10^{-4}	0.99199	5.1534×10^{-4}	0.98672
21	9.715×10^{-4}	0.99593	3.571×10^{-4}	0.99686	3.208×10^{-4}	0.99429
22	9.024×10^{-4}	0.9962	3.891×10^{-4}	0.99658	1.377×10^{-4}	0.98943
23	3.364×10^{-4}	0.99858	2.925×10^{-4}	0.99742	2.545×10^{-4}	0.95825
24	1.1×10^{-3}	0.9553	5.136×10^{-4}	0.99546	9.907×10^{-4}	0.97994
25	9.5×10^{-4}	0.99614	5.696×10^{-4}	0.99494	4.816×10^{-4}	0.99617
26	2×10^{-3}	0.99151	2.461×10^{-4}	0.99785	9.365×10^{-5}	0.9269
27	2.6×10^{-3}	0.98974	5.791×10^{-4}	0.99487	1.8×10^{-3}	0.9893
28	4×10^{-3}	0.984	4.845×10^{-4}	0.99573	2.582×10^{-4}	

It has been found that the accuracy of the developed model is very sensitive to the number of Hidden neurons. From Table 1 The best network structure was found to be [5× 23× 1] for the network predicts the axial velocity u, but for the network predicts v or k, the best structure is [5 × 26× 1]. R^2 and MSE values along typical ANN phases with variation in hidden

Journal of Information Systems Engineering and Management
2025, 10(4)
e-ISSN: 2468-4376
https://www.jisem-journal.com/

Research Article

neurons are depicted in Fig.4,5, and 6). The error must be continuously evaluated in each state of the neural network to choose the optimal network architecture.

Defining an error function - conventionally referred to as a loss function - is essential for this purpose. It can be used to calculate the model loss, allowing the weights to be updated to minimize the loss of the next evaluation.

It is worth noting that all stages have R2 values close to 1.0 and MSE values close to 0, with 23 and 26 hidden neurons shown in Figure 4 and 5,6 respectively by the dotted line.

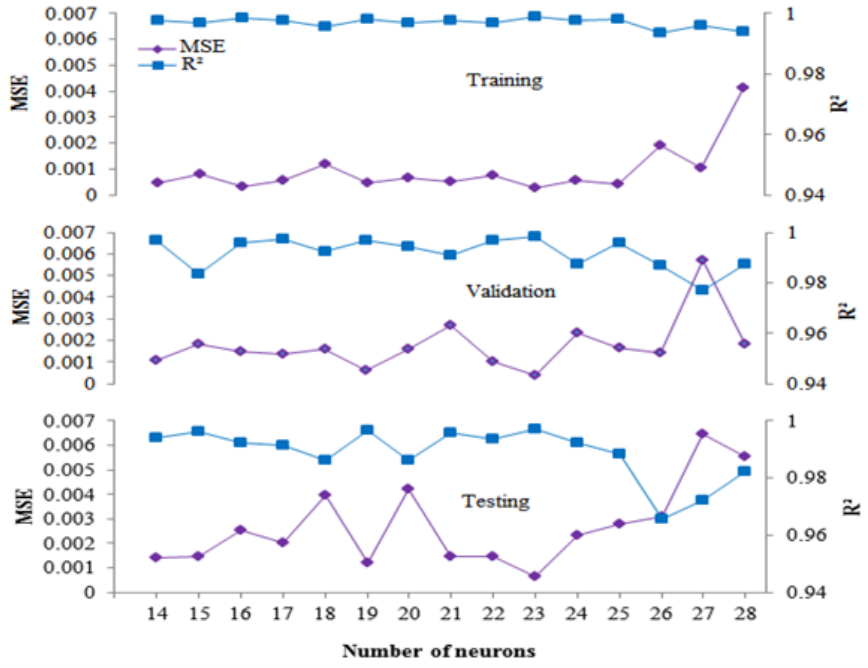

Figure 4: Variations in MSE and R2 values with the number of neurons, for axial velocity u

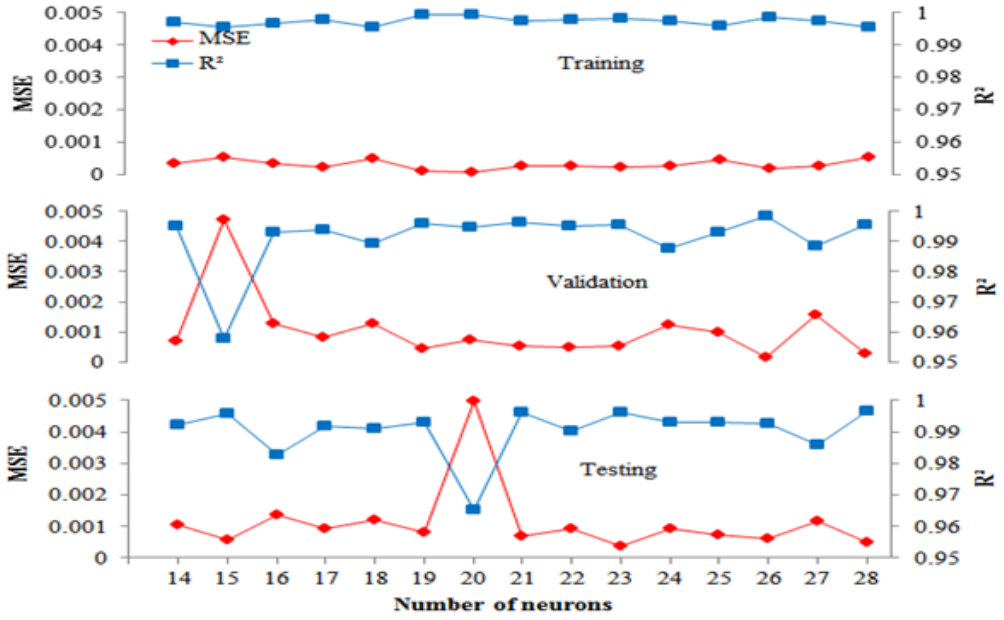

Figure 5: Variations in MSE and R2 values with the number of neurons for radial velocity v

Journal of Information Systems Engineering and Management
2025, 10(4)
e-ISSN: 2468-4376
https://www.jisem-journal.com/

Research Article

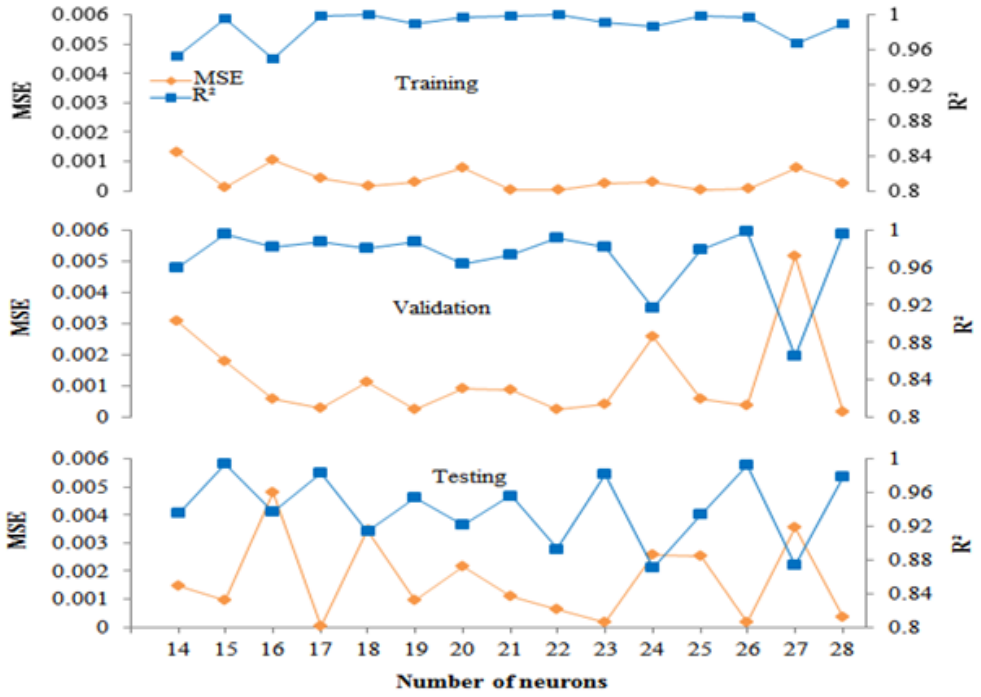

Figure 6: Variations in MSE and R2 values with number of neurons for Kinetic energy k

FFBPN Model prediction

Model training is carried out based on the ANN framework constructed above, and then a DNN model with high accuracy is obtained to predict the flow field distribution.

Fig. (7,8 and 9) represents a comparison between the ANN predicted values and experimental data for axial velocity u, radial velocity v, and kinetic energy k for the training set (70 %), the validation set (15%), and the test set (15%) of the datasets. That is, it represents a summary of the R^2 plots at the training, testing, and validation stages during the training process. An overall R^2 value of 0.9998 was obtained for the axial velocity u, 0.99785 for the radial velocity, and 0.99617 for the kinetic energy k. This indicates that the results are satisfactory because the overall R^2 score is close to 1.

It can be seen that the R^2 for the training, testing, and validation phase has high values in the range (0.992 - 0.999). That is, the data points are distributed around the line y = x, with some values deviating from the straight line, that is, the data points are distributed around the line y = x, with some values deviating from the straight line despite the existence of a relationship between experimental and expected, while maintaining a certain degree of linear

correlation and the ability of the model to reflect the main properties of the vortex flow field, i.e. goodness of fit. The expected and experimental values of u, v, and k are high.

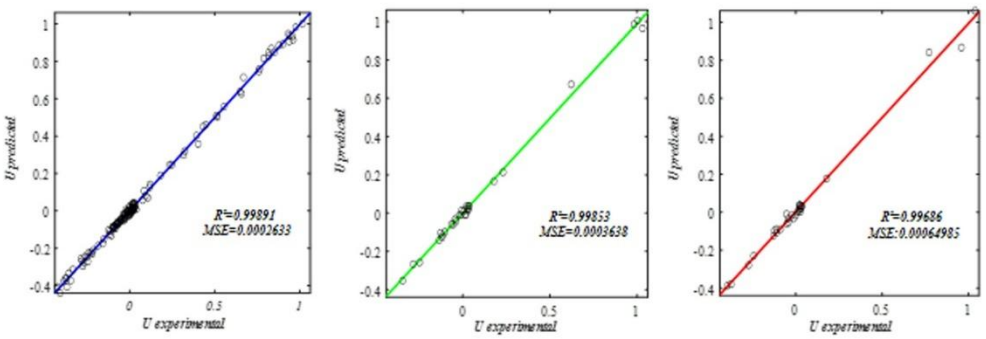

Training set validation set Testing set

Figure 7: Regression. Axial velocity u in training, validation, and testing

Journal of Information Systems Engineering and Management
2025, 10(4)
e-ISSN: 2468-4376
https://www.jisem-journal.com/

Research Article

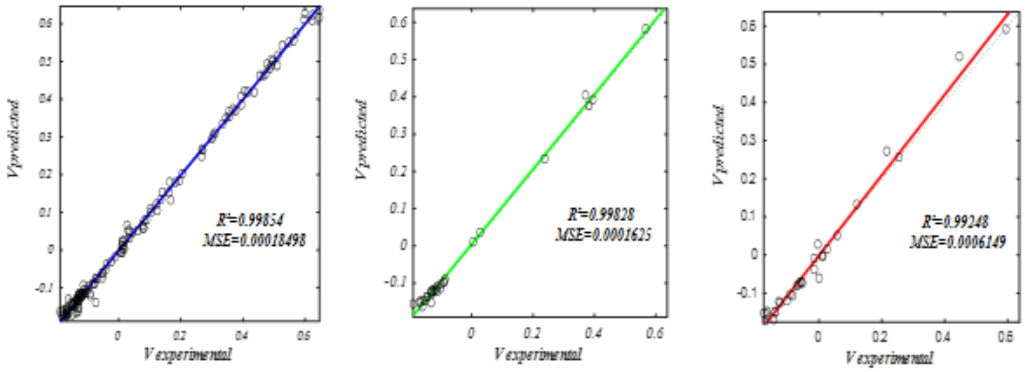

Training set *Validation set* *Testing set*

Figure 8: Regression. Radial velocity v in training, validation and testing

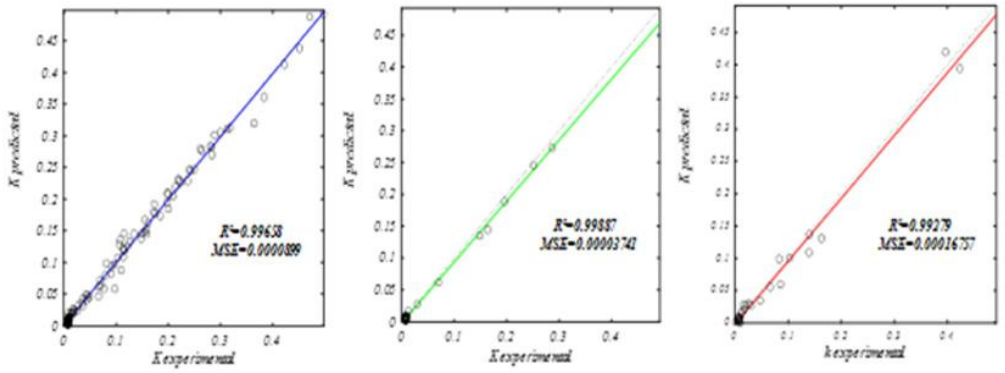

Training set *Validation set* *Testing set*

Figure 9: Regression. Kinetic energy *k*in training, validation and testing

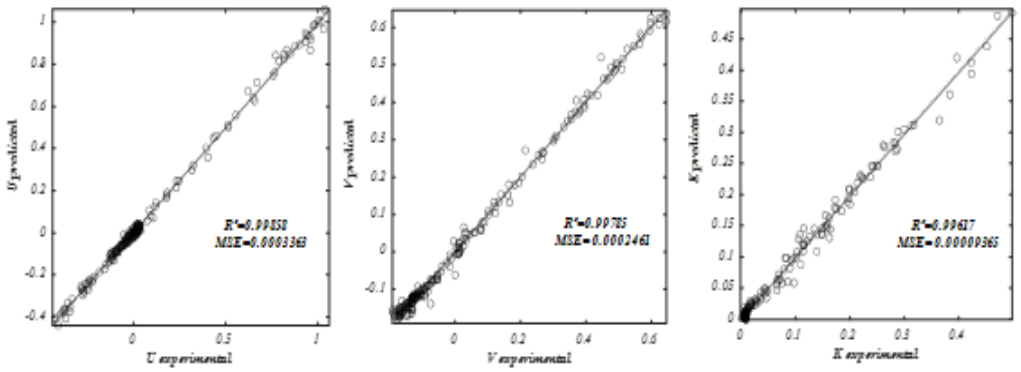

Axial velocity Radial velocity kinetic energy

Figure 10: Regression of all u, v and k

The neural network passes the data several times during the training process and stops when the lowest value is reached for mean square errors MSE. Fig. 11,12, and 13 show the evolution of the mean square errors during the training phase for axial velocity u, radial velocity v, and kinetic energy k, respectively.

Journal of Information Systems Engineering and Management
2025, 10(4)
e-ISSN: 2468-4376
https://www.jisem-journal.com/

Research Article

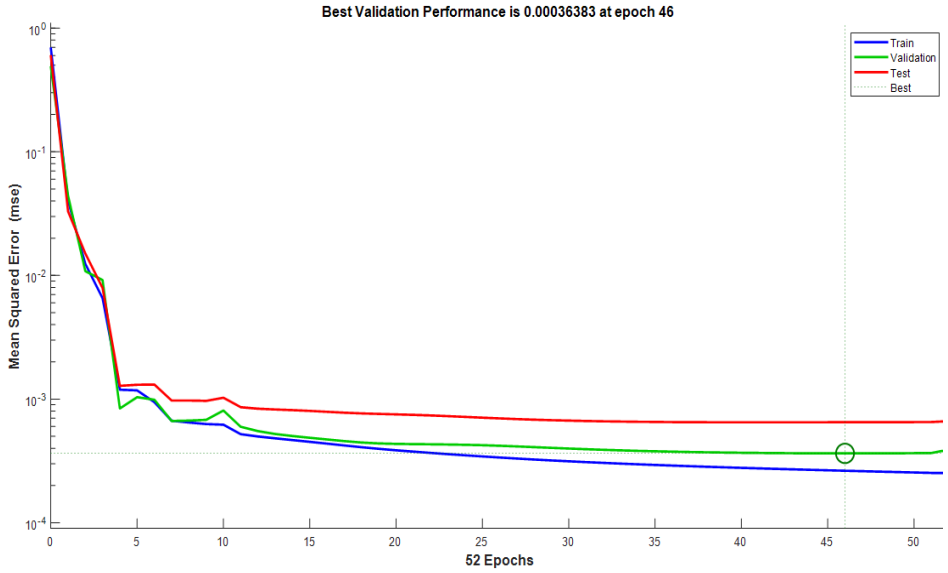

Figure 11: The evolution of the mean square errors during the training phase of axial velocity

We note from Fig.11 that the best value of the mean square error was in stage 46 of training, which was estimated at 3.6383*10.

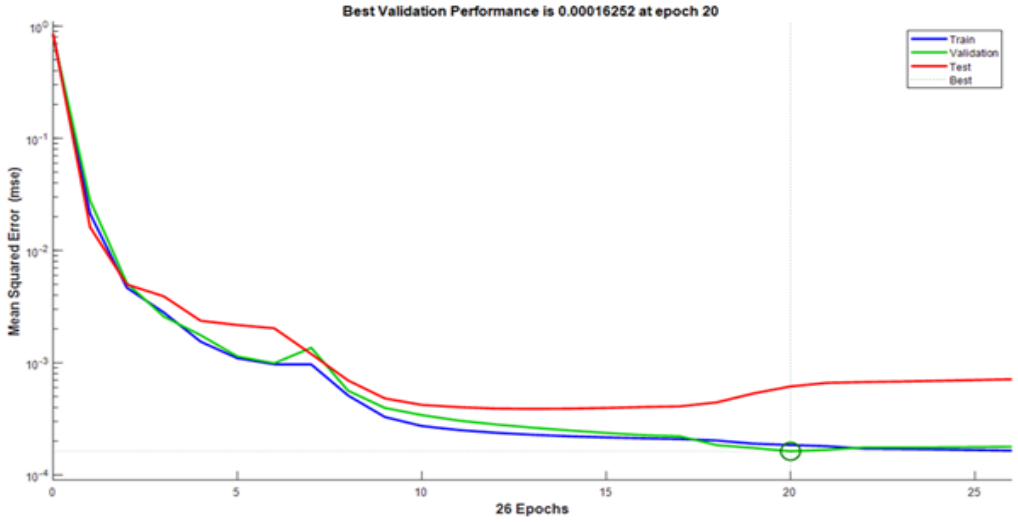

Figure 12: The evolution of the mean square errors during the training phase of radial velocity.

It can be seen from Fig.12 that The best validation performance was obtained at epoch 20, with the validation plot reaching its minimum MSE value of 0.00016252.

We note from Fig.13 that the best validation performance was obtained at epoch 21, with the validation plot reaching its minimum MSE value of 0.000037041.

Analysis of the results

Fig.14,15, and 16 show the fit and agreement between the experimental and predicted values for axial velocity, radial velocity, and kinetic energy. With the real and expected values agreeing, the relative R error approaches zero, representing the difference between them.

The introduction of rotor air through two concentric stages provides additional degrees of freedom for controlling the radial distribution of flow and vortex to achieve significantly different combustion characteristics, including flow and

Journal of Information Systems Engineering and Management
2025, 10(4)
e-ISSN: 2468-4376
https://www.jisem-journal.com/

Research Article

mixing patterns, turbulence levels, and different flame stability limits.

In Fig.14, negative axial velocity values in the vortex flow indicate the existence of reverse flow, or a recirculation zone, along the flow axis. The axial velocity is negative in this region because the axial direction of movement is opposite to the main flow direction. These regions also experience a decrease in flow velocity and an increase in airflow turbulence, which helps mix the reactants. This turbulence is used strategically to improve performance and increase efficiency. Fig.16 shows an increase in turbulent kinetic energy in these areas. As we move along the path of the combustion chamber (as shown in Fig.16), the turbulent kinetic energy gradually decreases until it reaches low or negligible levels, because the flame becomes stable at the end of the chamber.

At the vortex core level, the axial velocity is nearly zero. Thus, zero axial velocity at the vortex core is evidence of proper vortex flow formation. Execution III.4.2 describes the Feed feed-forward backpropagation Neural Network (FFBPN) prediction model. The model is trained based on the constructed Artificial Neural Network (ANN) framework to obtain a Deep Neural Network (DNN) model with high accuracy for predicting the flow field distribution. The comparison between the ANN predicted values and the experimental data for axial velocity (u), radial velocity (v), and kinetic energy (k) is represented in Fig.7, 8, and 9. These figures summarize the R-squared (R^2) plots at different stages of the training process, including the training set (70%), validation set (15%), and test set (15%) of the datasets. The overall R^2 value obtained for the axial velocity (u) is 0.9998, while the values for radial velocity (v) and kinetic energy (k) are 0.99785 and 0.99617 respectively. These high R^2 values indicate a strong relationship between the experimental and predicted values, reflecting the model's ability to accurately represent the main properties of the vortex flow field. Furthermore, the mean square errors (MSE) during the training phase are illustrated in Fig.11,12, and 13, showing the evolution of MSE for axial velocity, radial velocity, and kinetic energy.

Based on the results, it is evident that the FFBPN model demonstrates high accuracy and validity, supported by the R^2 values and low MSE. The presence of reverse flow or recirculation zones along the flow axis is indicated by negative axial velocity values in the vortex flow, contributing to improved performance and efficiency through strategic use of airflow turbulence. Additionally, the analysis of the radial velocity and kinetic energy provides insights into the flow characteristics at different locations within the combustion chamber. The predicted values show good agreement with the experimental data, with negligible relative errors.

In conclusion, this chapter emphasizes the significance of predicting swirling flow characteristics using the FFBPN model and highlights the accuracy and validity of the model based on the obtained results. It is noted that the accuracy of the predicted output is influenced by the number of neurons in the model. Al velocity transitions from negative to positive values in the vortex flow when moving from the recirculation zones to areas farther from the vortex core. On the other hand, high positive values indicate a large velocity gradient and high turbulence intensity, which can lead to strong mass and energy exchange. As for the radial velocity, it is practically zero at the recirculation zo

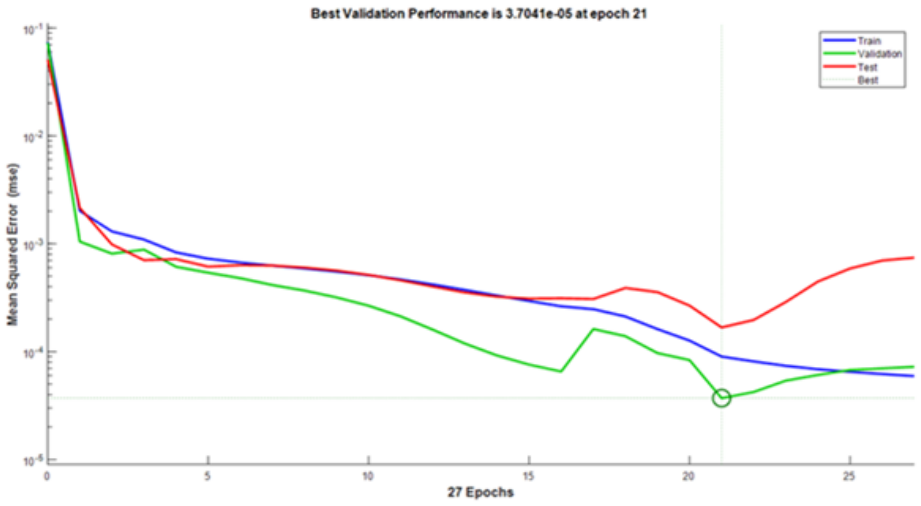

Figure 13: The evolution of the mean square errors during the training phase. Of kinetic energy

Journal of Information Systems Engineering and Management
2025, 10(4)
e-ISSN: 2468-4376
https://www.jisem-journal.com/

Research Article

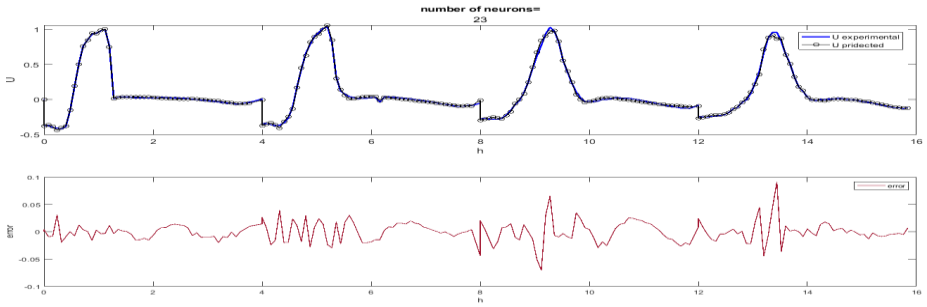

Figure 14: Comparison of axial velocity u from prediction and experiment at different locations.

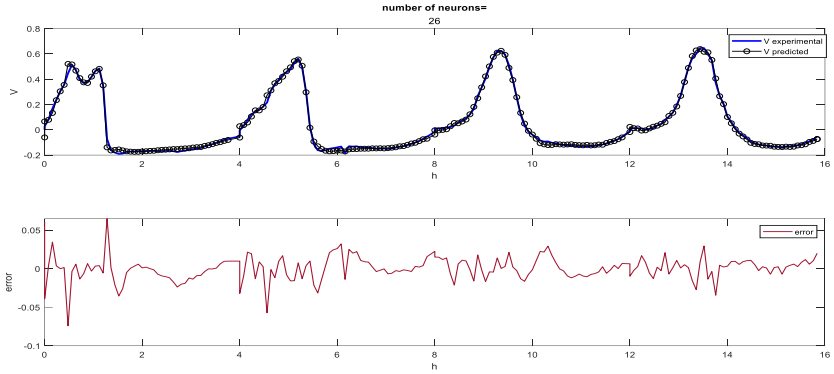

Figure 15: Comparison of radial velocity v from prediction and experiment at different **locations**

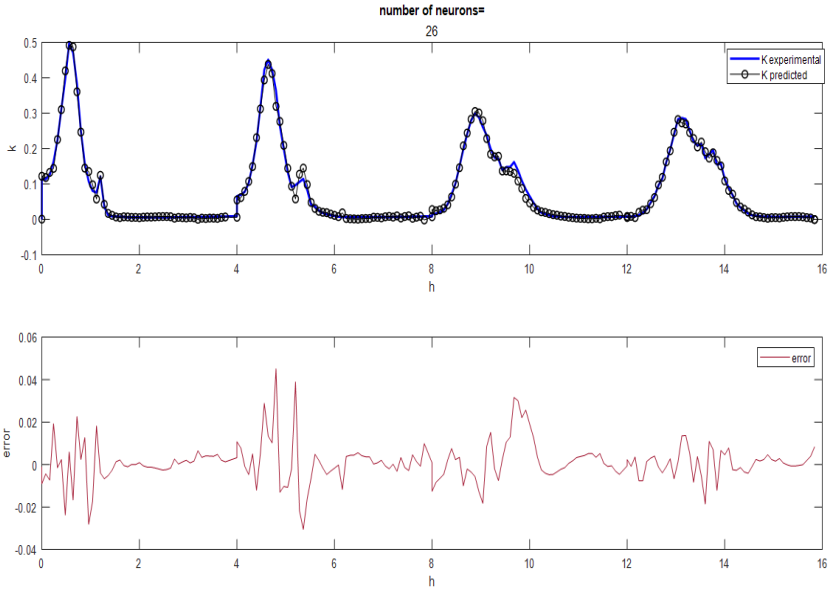

Figure16: Compare kinetic energy k from prediction and experiment at different locations

CONCLUSION

This study developed an artificial neural network model to predict the characteristics of swirling flow and evaluate its effectiveness. Swirl (vortex) flow plays a key role in industrial combustion systems by enhancing fuel–air mixing, ensuring uniform temperature distribution, and recirculating unburned gases to the flame. Within the recirculation zone, flow velocity decreases while turbulence intensity increases, leading to negative radial and axial velocity components.

The proposed Feedforward Backpropagation Neural Network (FFBPNN) demonstrated high accuracy in predicting eddy flow characteristics, achieving low mean squared error values. Prediction accuracy was found to be strongly influenced by the number of neurons in the hidden layer. The model not only reproduced vortex flow fields from known datasets but also extrapolated them under previously unseen inlet conditions. Its computational efficiency, versatility, and rapid

response make it well-suited for three-dimensional, multipara meter, and multi-objective flow field prediction.

This work focused on non-reacting swirling flows; future extensions will incorporate fuel–air ratio and temperature as inputs to predict turbulent reacting flow characteristics, thereby reducing reliance on costly experimental methods. Further research will also investigate coupled prediction between combustion species concentration fields and swirling flow structures.

REFERENCES

[1] Escudier, M., & Keller, J. (1985). Recirculation in swirling flow-a manifestation of vortex breakdown. *AIAA journal*, *23*(1), 111-116.

[2] Guedot, L. (2015). Développement de méthodes numériques pour la caractérisation des grandes structures tourbillonnaires dans les brûleurs aéronautiques : application aux systèmes d'injection multi-points INSA de Rouen].

[3] Leuckel, W., & Fricker, N. (1976). Characteristics of swirl-stabilized natural gas flames. I. Different flame types and their relation to flow and mixing patterns. *J. Inst. Fuel;(United Kingdom)*, *49*(399).

[4] Mathur, M., & NR, M. (1967). Swirling air jets issuing from vane swirlers. 1. Free jets. *Journal of the Institute of Fuel*, *40*(316), 214-&.

[5] Merkle, K., Bu¨ chner, H., Zarzalis, N., & Sara, O. N. (2003). Influence of co and counter swirl on lean stability limits of an airblast nozzle. Turbo Expo: Power for Land, Sea, and Air,

[6] Moayedi, H., Aghel, B., Vaferi, B., Foong, L. K., & Bui, D. T. (2020). The feasibility of Levenberg–Marquardt algorithm combined with imperialist competitive computational method predicting drag reduction in crude oil pipelines. *Journal of Petroleum Science and Engineering*, *185*, 106634.

[7] O'Doherty, T., & Lucca-Negro, O. (2001). Vortex breakdown: a review. *Progress in Energy and Combustion Science*, *27*(4), 431-481.

[8] Schmittel, P., Günther, B., Lenze, B., Leuckel, W., & Bockhorn, H. (2000). Turbulent swirling flames: Experimental investigation of the flow field and formation of nitrogen oxide. *Proceedings of the Combustion Institute*, *28*(1), 303-309.

[9] Shaik, N. B., Pedapati, S. R., Taqvi, S. A. A., Othman, A., & Dzubir, F. A. A. (2020). A feed-forward back propagation neural network approach to predict the life condition of crude oil pipeline. *Processes*, *8*(6), 661.

[10] Sheen, H. J., Chen, W., Jeng, S., & Huang, T. (1996). Correlation of swirl number for a radial-type swirl generator. *Experimental thermal and fluid science*, *12*(4), 444-451.

[11] Syred, N. (2006). A review of oscillation mechanisms and the role of the precessing vortex core (PVC) in swirl combustion systems. *Progress in Energy and Combustion Science*, *32*(2), 93-161.

[12] Zabihi, R., Mowla, D., & Karami, H. R. (2019). Artificial intelligence approach to predict drag reduction in crude oil pipelines. *Journal of Petroleum Science and Engineering*, *178*, 586-593.